ANALYSIS AND DESIGN ASPECTS OF MOMENT-RESISTING, BEAM-TO-COLUMN, TIMBER CONNECTIONS WITH INCLINED THREADED RODS: FROM FASTENER LEVEL TO CONSTRUCTION LEVEL

Haris Stamatopoulos[1], Osama Abdelfattah Hegeir [2], Kjell Arne Malo [3]

ABSTRACT: Moment-resisting timber frames (MRTFs) can be an alternative load-carrying system for mid-rise buildings, compared to systems based on walls or diagonals. The response of MRTFs depends largely on their connections. This paper provides an overview of analysis and design aspects of connections for MRTFs based on inclined threaded rods. Simplified expressions are provided for the properties of such connections and for the properties of threaded rods. Finally, the effects of connection's stiffness variability are explored. It is shown that this variability can result in increased values of actions compared to the values obtained by use of mean connection stiffness.

KEYWORDS: Moment-resisting connections, Moment-resisting frames, Threaded rods, Stiffness variability

1 INTRODUCTION

Moment-resisting timber frames (MRTFs) can reduce the need for bracing by shear walls or diagonal elements and allow for greater architectural flexibility in mid-rise buildings. The response of MRTFs depends on the properties of their connections, especially with respect to the serviceability aspects, see e.g.[1]. Moreover, MRTFs are statically indeterminate structures and the magnitude and distribution of internal forces and moments at the Ultimate Limit State, depend on the stiffness of their connections. The variability of the connections' stiffness can also significantly influence the internal forces and moments as will be shown in Section 4.

A concept for a moment-resisting connection with inclined threaded rods is presented in Figure 1. The rods are inserted with an inclination in pre-drilled holes in the beam and the column and jointed by use of metallic coupling parts. In the prototype tests for this concept [2], beams and columns were made of glued-laminated timber (glulam) and purpose-made steel rings were used as the coupling parts, see Figure 1. To allow fastening of rods to the steel rings, threaded rods with metric thread at their end are used, as shown in Figure 1. The use of steel brackets or plates and friction bolts can be an alternative to steel rings, see for example [3].

As shown in Figure 1, the coupling parts are connected to the column by use of a pair of inclined threaded rods (rods c1-c2 at the top and rods c3-c4 at the bottom). Due to rod inclination and the presence of shear forces, a load situation consisting of both axial and lateral forces occurs in the rods. However, the rods will mainly experience axial forces since their axial stiffness is much greater than the lateral one. The transfer of forces in this configuration resembles the transfer of forces in a truss system where all members are axially loaded. Therefore, the lateral forces in the rods c1, c2, c3 and c4 may be neglected.

The rods in the beam are inserted at a small angle. Rods parallel to the grain are vulnerable to cracks since a single crack along the grain might lead to a considerable loss of strength if the crack occurs in the same plane as the rod. Therefore, the beam is connected to the coupling parts by use of threaded rods (b1 and b2) inserted at a small angle to the grain, i.e. 5°-10°, see Figure 1. Greater angle should be avoided as it would also result in high lateral forces in the threaded rods and therefore smaller stiffness.
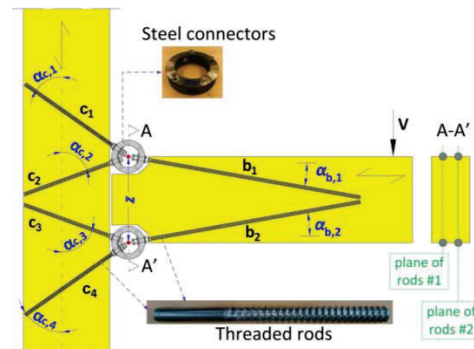

Figure 1: *Moment-resisting connection with inclined rods*

This paper consists of two parts:

- In the first part (Sections 2 and 3), analytical expressions are provided for the estimation of the properties of a connection as shown in Figure 1 and for the rods, based on recent publications;
- In the second part (Section 4) a preliminary study regarding the effects of connection stiffness variability on response of MRTFs is presented.

[1] Haris Stamatopoulos, haris.stamatopoulos@ntnu.no
[2] Osama Abdelfattah Hegeir, osama.a.s.a.hegeir@ntnu.no
[3] Kjell Arne Malo, kjell.malo@ntnu.no
Norwegian University of Science and Technology (NTNU)

2 CONNECTION PROPERTIES

2.1 STIFFNESS

The connection in Figure 1 can be considered as a system of rotational springs in series consisting of: a) the connection of rods c_1-c_4 to the column with spring constant $K_{\theta,c}$, b) the connection of rods b_1-b_2 to the beam with spring constant $K_{\theta,b}$ and c) the connectors with spring constant $K_{\theta,con}$. Therefore, the rotational stiffness of the connection can be determined by Eq.(1). The geometry is given in Figure 2. In [4], Eqs.(2)-(3) were derived by use of the component method and validated by experimental results. The compliance S-terms (Eqs.(4)-(7)) are given as functions of the axial stiffness ($K_{ax,i}$) and lateral stiffness ($K_{v,i}$) of the rods and the rod-to-grain angles (Eq.(8)). In Figure 2 and Eqs.(2)-(3), the lever arm is assumed the same on the beam and the column side ($z_b = z_c = z$). However, Eqs.(2)-(3) can also be applied for different lever arms. Eqs.(2)-(3) depend also on the moment to shear ratio ($L_v = M/V$) which is not known - a priori - in the structural analysis and approximations are needed, see also Eqs.(9)-(12). Eqs.(1)-(8) apply per plane of rods.
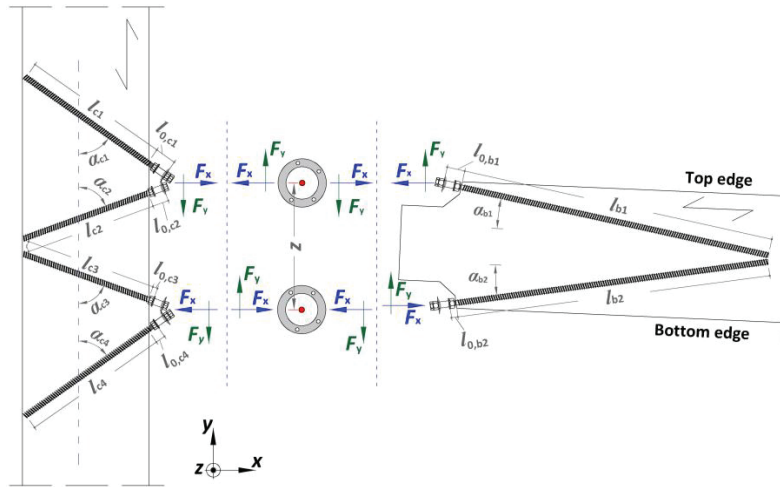

Figure 2: *Forces and geometry of a moment resisting connection with inclined threaded rods*

$$K_\theta = \left(1/K_{\theta,c} + 1/K_{\theta,b} + 1/K_{\theta,con}\right)^{-1} \tag{1}$$

$$K_{\theta,c} = \frac{z^2}{\left(S_{xx,c}^{(c1-c2)} + S_{xx,c}^{(c3-c4)}\right) + \left(S_{xy,c}^{(c3-c4)} - S_{xy,c}^{(c1-c2)}\right) \cdot z/(2 \cdot L_v)} \tag{2}$$

$$K_{\theta,b} = \frac{z^2}{\left(S_{xx,b1} + S_{xx,b2}\right) + \left(S_{xy,b2} - S_{xy,b1}\right) \cdot z/(2 \cdot L_v)} \tag{3}$$

$$S_{xx,c}^{(c1-c2)} = \frac{c_{c1}^2/K_{ax,c2} + c_{c2}^2/K_{ax,c1}}{(c_{c1} \cdot s_{c2} + c_{c2} \cdot s_{c1})^2} \;;\; S_{xx,c}^{(c3-c4)} = \frac{c_{c3}^2/K_{ax,c4} + c_{c4}^2/K_{ax,c3}}{(c_{c3} \cdot s_{c4} + c_{c4} \cdot s_{c3})^2} \tag{4}$$

$$S_{xy,c}^{(c1-c2)} = \frac{c_{c1} \cdot s_{c1}/K_{ax,c2} - c_{c2} \cdot s_{c2}/K_{ax,c1}}{(c_{c1} \cdot s_{c2} + c_{c2} \cdot s_{c1})^2} \;;\; S_{xy,c}^{(c3-c4)} = \frac{c_{c3} \cdot s_{c3}/K_{ax,c4} - c_{c4} \cdot s_{c4}/K_{ax,c3}}{(c_{c3} \cdot s_{c4} + c_{c4} \cdot s_{c3})^2} \tag{5}$$

$$S_{xx,b1} = s_{b1}^2/K_{v,b1} + c_{b1}^2/K_{ax,b1} \;;\; S_{xx,b2} = s_{b2}^2/K_{v,b2} + c_{b2}^2/K_{ax,b2} \tag{6}$$

$$S_{xy,b1} = s_{b1} \cdot c_{b1} \cdot \left(1/K_{v,b1} - 1/K_{ax,b1}\right) \;;\; S_{xy,b2} = s_{b2} \cdot c_{b2} \cdot \left(1/K_{ax,b2} - 1/K_{v,b2}\right) \tag{7}$$

$$c_i = \cos\alpha_i \;;\; s_i = \sin\alpha_i \;;\; L_v = M/V \tag{8}$$

Neglecting the shear term in Eqs.(2)-(3) results in the following crude approximations:

$$K_{\theta,c} \approx z^2/\left(S_{xx,c}^{(c1-c2)} + S_{xx,c}^{(c3-c4)}\right) \tag{9}$$

$$K_{\theta,b} \approx z^2/\left(S_{xx,b1} + S_{xx,b2}\right) \tag{10}$$

Assuming further that the rods are inserted at equal angles in the column ($\alpha_{c,1} = \alpha_{c,2} = \alpha_{c,3} = \alpha_{c,4} = \alpha_c$) and the beam ($\alpha_{b,1} = \alpha_{b,2} = \alpha_b$) and that they approximately have equal stiffness ($K_{ax,c1} = K_{ax,c2} = K_{ax,c3} = K_{ax,c4} = K_{ax,c}$, $K_{ax,b1} = K_{ax,b2} = K_{ax,b}$, $K_{v,b1} = K_{v,b2} = K_{v,b}$), Eqs.(9)-(10) can be further simplified as follows:

$$K_{\theta,c} \approx z^2 \cdot K_{ax,c} \cdot s_c{}^2 \qquad (11)$$

$$K_{\theta,b} \approx \frac{z^2 \cdot K_{ax,b}/2}{\left(K_{ax,b}/K_{v,b}\right) \cdot s_b{}^2 + c_b{}^2} \qquad (12)$$

2.2 FORCES IN THE RODS

The forces in each rod can also be determined by use of the component method [4]. The rods on the column-side are mainly axially loaded and the forces are equal to:

$$\begin{Bmatrix} F_{ax,c1} \\ F_{ax,c2} \end{Bmatrix} = \frac{1}{n} \cdot \begin{Bmatrix} \dfrac{c_{c2} + s_{c2} \cdot z/(2 \cdot L_v)}{c_{c1} \cdot s_{c2} + c_{c2} \cdot s_{c1}} \\ \dfrac{c_{c1} - s_{c1} \cdot z/(2 \cdot L_v)}{c_{c1} \cdot s_{c2} + c_{c2} \cdot s_{c1}} \end{Bmatrix} \cdot \frac{M}{z} \qquad (13)$$

$$\begin{Bmatrix} F_{ax,c3} \\ F_{ax,c4} \end{Bmatrix} = -\frac{1}{n} \cdot \begin{Bmatrix} \dfrac{c_{c4} - s_{c4} \cdot z/(2 \cdot L_v)}{c_{c3} \cdot s_{c4} + c_{c4} \cdot s_{c3}} \\ \dfrac{c_{c3} + s_{c3} \cdot z/(2 \cdot L_v)}{c_{c3} \cdot s_{c4} + c_{c4} \cdot s_{c3}} \end{Bmatrix} \cdot \frac{M}{z} \qquad (14)$$

On the beam-side, the rods are subjected to combined axial and lateral loading [4]:

$$\begin{Bmatrix} F_{ax,b1} \\ F_{v,b1} \end{Bmatrix} = \frac{1}{n} \cdot \begin{Bmatrix} c_{b1} + s_{b1} \cdot z/(2 \cdot L_v) \\ -s_{b1} + c_{b1} \cdot z/(2 \cdot L_v) \end{Bmatrix} \cdot \frac{M}{z} \qquad (15)$$

$$\begin{Bmatrix} F_{ax,b2} \\ F_{v,b2} \end{Bmatrix} = -\frac{1}{n} \cdot \begin{Bmatrix} c_{b2} + s_{b2} \cdot z/(2 \cdot L_v) \\ -s_{b2} + c_{b2} \cdot z/(2 \cdot L_v) \end{Bmatrix} \cdot \frac{M}{z} \qquad (16)$$

Eqs.(13)-(16) can be used in the corresponding design checks for the rods, see also Section 3. The parameter n is the number of planes of rods.

2.3 PANEL ZONE

Horizontal forces result in high shear stresses in the panel zone of the column, i.e. the region between rods c1-c2 and c3-c4. Moreover, stresses perpendicular to grain occur around the threaded rods. The combination of tensile stresses perpendicular to grain and shear stresses is unfavourable due to their high degree of interaction [5] and may cause fracture in the panel zone, as shown in Figure 3. Thus, the panel zone must be designed with sufficient strength against combined shear and tension perpendicular to grain. If the rods are long and cross the entire height of the column they act as reinforcements [6], increasing the capacity of the panel zone.
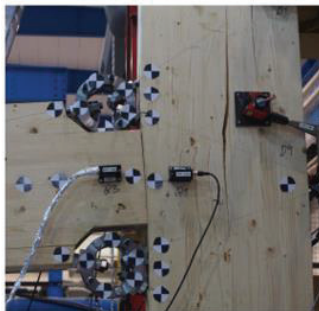

Figure 3: *Fracture in the panel zone due to combined shear and tension perpendicular to grain (Photo: [2])*

3 FASTENER PROPERTIES

The properties of threaded rods are necessary inputs for the properties of the entire connection. The axial stiffness of a threaded rod is given by:

$$K_{ax} = \frac{K_{ser,ax} \cdot K_{ax,l0}}{K_{ser,ax} + K_{ax,l0}} \qquad (17)$$

where $K_{ser,ax}$ is the withdrawal stiffness and $K_{ax,l0}$ is the axial stiffness of the non-embedded part of the rod:

$$K_{ax,l0} = A_{net} \cdot E_s/l_0 \qquad (18)$$

where $E_s = 210000$ N/mm² is the modulus of elasticity of steel, A_{net} is the net cross-sectional area and l_0 is the non-embedded length of the rod. Eq.(19) provides an approximation for $K_{ser,ax}$ (in N/mm) as function of the outer-thread diameter d (in mm), the rod-to-grain angle α, the mean density ρ_m (in kg/m³) and the embedment length l (in mm). Eq.(19) was derived in [7] by use of non-linear regression on experimental results for threaded rods with diameters 16-20 mm embedded in softwood, see [8-10].

$$K_{ser,ax} \approx \frac{50000 \cdot \left(\dfrac{d}{20}\right)^2 \cdot \left(\dfrac{\rho_m}{470}\right)^2 \cdot k_{length,K}}{0.40 \cdot \cos^{2.3}\alpha + \sin^{2.3}\alpha} \qquad (19)$$

$$k_{length,K} = \min\left[(l/300)^{3/4}, 1\right] \qquad (20)$$

The stiffness of a laterally loaded threaded rod can be determined by Eq.(21). Eq.(21) is derived by modelling the rod as a beam on elastic foundation assuming that rotation is restrained at the loading point, see in detail [7]:

$$K_v = \frac{3 \cdot k_v \cdot l_{ch}}{\lambda_0{}^3 + 3 \cdot \lambda_0{}^2 + 3 \cdot \lambda_0 + 3} \qquad (21)$$

$$\lambda_0 = l_0/l_{ch} \; ; \; l_{ch} = \sqrt[4]{4 \cdot E_s \cdot I_s/k_v} \qquad (22)$$

The parameter $I_s \approx \pi \cdot d_1{}^4/64$ is the 2nd moment of area and d_1 is the core diameter of the rod. The parameter k_v is the foundation modulus (i.e. stiffness per unit length) of a laterally loaded rod. According to Eqs.(3),(6),(7) and (12), the lateral stiffness of a rod is an input parameter for the rotational stiffness on the beam-side. There the rods are inserted at small angles to grain and therefore the lateral foundation modulus may be approximately taken as the foundation modulus perpendicular to the grain. Based on an experimental study of laterally loaded rods with $d = 22$ mm embedded in glulam made of pine and spruce [11] an approximate value of $k_v \approx 300$ N/mm² may be used.

A power criterion is often used - as an approximation - to determine the capacity of fasteners subjected to combined axial force (F_{ax}) and lateral force (F_v), i.e.:

$$\left(\frac{F_{ax}}{F_{ax,R}}\right)^q + \left(\frac{F_v}{F_{v,R}}\right)^q \leq 1 \qquad (23)$$

In Eq.(23), $F_{ax,R}$ and $F_{v,R}$ are the axial and lateral capacity of a fastener respectively. According to EN 1995-1-1 [12], a quadratic failure criterion applies for screws, i.e. $q = 2$. The quadratic criterion has provided safe-sided predictions for long screws (i.e. with steel failure being

more critical than withdrawal) inserted perpendicular to grain [13] and for glued-in rods parallel to grain [14]. The rods on the beam side are subjected to both lateral and axial forces and therefore their capacity should be checked by use of a criterion that considers the interaction of forces, as the one given by Eq.(23). On the other hand, the rods in the column are mainly axially loaded (i.e. $F_{v,ci} \approx 0$) as explained in Section 1 and therefore in this case Eq.(23) reduces to: $|F_{ax,ci}| \leq F_{ax,R}$.

4 STIFFNESS VARIABILITY EFFECTS

MRTFs are statically indeterminate systems, and the distribution of the internal actions depends on the stiffness of their elements and connections. The internal forces and moments are typically determined by use of mean stiffness values in the structural analysis. However, the inherent variability of the connection stiffness can result in variations of internal forces and moments, compared to the expected values obtained by use of mean stiffness values. In this section, the effects of connection stiffness variability are explored by use of a simple beam model with semi-rigid end restrains (Section 4.1) and by linear-elastic Finite Element simulations of MRTFs with semi-rigid moment connections (Section 4.2).

4.1 BEAM MODEL

A beam with semi-rigid end restrains (Figure 4) subjected to uniformly distributed load q is used here -as a simple example- to study the effects of the connections' stiffness variability. The connections are represented by linear-elastic rotational springs with spring constants $K_{\theta,1}$ and $K_{\theta,2}$ which can be expressed in dimensionless form-by dividing by the beam stiffness-as follows:

$$k_1 = \frac{K_{\theta,1}}{(EI/L)} \; ; \; k_2 = \frac{K_{\theta,2}}{(EI/L)} \quad (24)$$
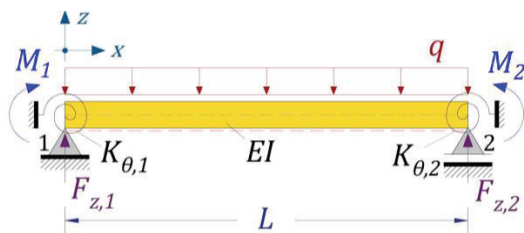
Figure 4: *Simply supported beam with semi-rigid end restrains*

The moments and the vertical forces at the beam ends can be expressed as functions of k_1 and k_2 as follows:

$$M_1 = -\frac{q \cdot L^2}{12} \cdot \frac{k_1 \cdot (k_2 + 6)}{k_1 \cdot k_2 + 4 \cdot (k_1 + k_2) + 12} \quad (25)$$

$$F_{z,1} = \frac{q \cdot L}{2} \cdot \frac{k_1 \cdot k_2 + 5 \cdot k_1 + 3 \cdot k_2 + 12}{k_1 \cdot k_2 + 4 \cdot (k_1 + k_2) + 12} \quad (26)$$

$$M_2 = -\frac{q \cdot L^2}{12} \cdot \frac{k_2 \cdot (k_1 + 6)}{k_1 \cdot k_2 + 4 \cdot (k_1 + k_2) + 12} \quad (27)$$

$$F_{z,2} = \frac{q \cdot L}{2} \cdot \frac{k_1 \cdot k_2 + 3 \cdot k_1 + 5 \cdot k_2 + 12}{k_1 \cdot k_2 + 4 \cdot (k_1 + k_2) + 12} \quad (28)$$

The maximum span moment can be simply written as function of the forces and moments:

$$M_{span} = M_1 + \frac{F_{z,1}^2}{2 \cdot q} = M_2 + \frac{F_{z,2}^2}{2 \cdot q} \quad (29)$$

By letting $k_1 = k_2 = k_{mean}$, the moments and the reactions at the supports become equal ($M_1 = M_2 = M_{end}$ and $F_{z,1} = F_{z,2} = F_z$):

$$M_{end}(k_1 = k_2 = k_{mean}) = -\frac{q \cdot L^2}{12} \cdot \frac{k_{mean}}{k_{mean} + 2} \quad (30)$$

$$F_z(k_1 = k_2 = k_{mean}) = \frac{q \cdot L}{2} \quad (31)$$

$$M_{span}(k_1 = k_2 = k_{mean}) = \frac{q \cdot L^2}{24} \cdot \frac{k_{mean} + 6}{k_{mean} + 2} \quad (32)$$

For each realization of the connections' stiffness, the ratios between the actual action divided by the corresponding values by use of mean stiffness values were calculated, as specified by Eqs.(33)-(37). These ratios express the deviation between a realization (numerator) and the corresponding value obtained by static analysis by use of mean stiffness (denominator) and they depend only on the normalized stiffness values given by Eq.(24).

$$n_{M,end,1} = \frac{|M_1(k_1, k_2)|}{|M_{end}(k_1 = k_2 = k_{mean})|} \quad (33)$$

$$n_{M,end,2} = \frac{|M_2(k_1, k_2)|}{|M_{end}(k_1 = k_2 = k_{mean})|} \quad (34)$$

$$n_{M,span} = \frac{M_{span}(k_1, k_2)}{M_{span}(k_1 = k_2 = k_{mean})} \quad (35)$$

$$n_{V,end,1} = \frac{F_{z,1}(k_1, k_2)}{F_z(k_1 = k_2 = k_{mean})} \quad (36)$$

$$n_{V,end,2} = \frac{F_{z,2}(k_1, k_2)}{F_z(k_1 = k_2 = k_{mean})} \quad (37)$$

In other words, the ratios by Eqs.(33)-(37) multiplied by the internal forces and moments by use of mean stiffness provide the actual internal forces and moments. Therefore, to get an indication of the unfavourable effect of stiffness variability on the internal forces and moments, it makes sense to consider an upper percentile value of these ratios, e.g. the 95th or 98th percentile. Thus, the variability of the ratios by Eqs.(33)-(37) is important. To study the effects of stiffness variability, realizations of normalized stiffness values k_1 and k_2 were generated. Note that the variability of parameters k_1 and k_2 results from the variability of the properties of the connection (K_θ) and the material (E). Here, for simplicity k_1 and k_2 were assumed as the random variables instead of K_θ and E separately. Due to the lack of data with respect to the distribution of the connection stiffness K_θ, two different distributions were assumed: namely normal and

lognormal distribution. Figure 6 shows an example of the distribution of the ratio $n_{M,end}$ (Eq.(33) or Eq.(34)) assuming that k_1 and k_2 are either normally or lognormally distributed. The distribution of the output variable $n_{M,end}$ is fairly similar for both assumptions. This observation holds true for relatively small values of k_{mean} and $CoV(k)$ and for the other output variables ($n_{M,span}$ or $n_{V,end}$) with some small deviations.
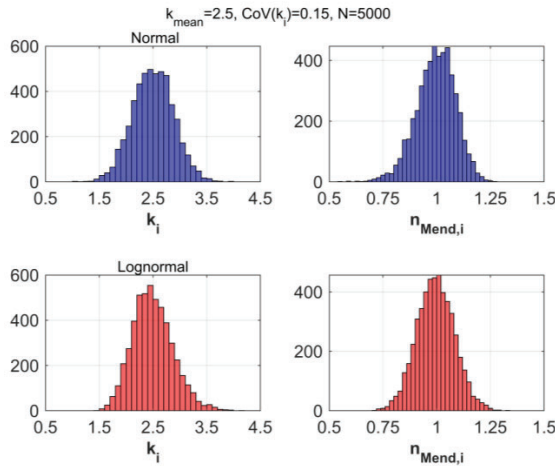

Figure 5: *Distribution of $n_{M,end}$ (right) for normal (up-left) and lognormal (bottom-left) distribution of k_1 and k_2 (example here for $k_{mean} = 2.5$ and $CoV(k) = 0.15$)*

Given that the distribution of the output variables (Eqs.(33)-(37)) is fairly similar for either normal or lognormal distribution of the input variables k_1 and k_2, only results assuming normal distribution of k_1 and k_2 are presented further. The mean value is denoted k_{mean} and the coefficient of variation is denoted $CoV(k)$, thus:

$$k_1 = N(k_{mean}, CoV(k)) \qquad (38)$$

$$k_2 = N(k_{mean}, CoV(k)) \qquad (39)$$

Figure 6 shows the ratio $n_{M,end}$ according to Eq.(33) or Eq.(34) for varying values of k_{mean} based on 5000 realizations per k_{mean}-value. Figure 7 shows the corresponding results for $n_{M,span}$ (Eq.(35)) and Figure 8 for $n_{V,end}$ (Eq.(36) or Eq.(37)). All Figures are plotted for $CoV(k) = 0.15$. Such coefficient of variation has been observed for the rotational stiffness of connections with glulam beams and columns and inclined threaded rods as shown in Figure 1 [15]; however the sample size was small and this number is only used as indicative.

The 95th and the 98th percentiles are also provided in the Figures together with the theoretical estimations that correspond to normal distribution: $X_{95\%} = X_{mean} \cdot (1 + 1.645 \cdot CoV[X])$ and $X_{98\%} = X_{mean} \cdot (1 + 2.054 \cdot CoV[X])$. As shown in the Figures, these estimations are in good agreement with the percentiles of each sample.
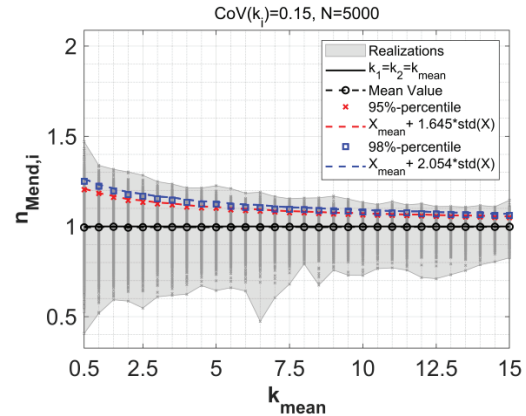
Figure 6: *Ratio $n_{M,end}$ for varying k_{mean} and $CoV(k_i) = 0.15$ (5000 realizations per k_{mean} value, assuming that k_1 and k_2 are normally distributed)*
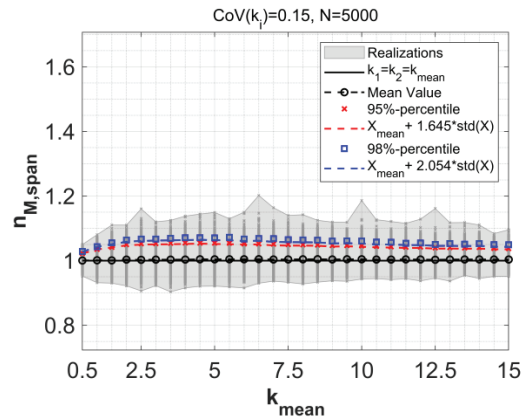
Figure 7: *Ratio $n_{M,span}$ for varying k_{mean} and $CoV(k_i) = 0.15$ (5000 realizations per k_{mean} value, assuming that k_1 and k_2 are normally distributed)*
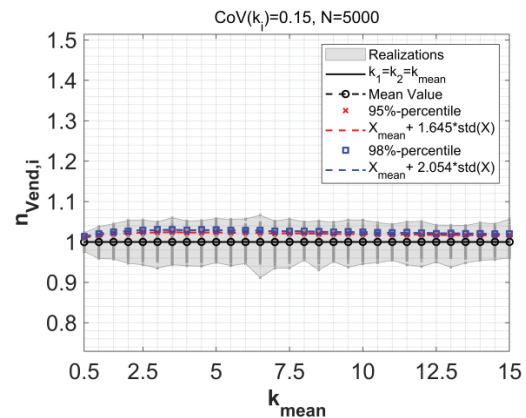
Figure 8: *Ratio $n_{V,end}$ for varying k_{mean} and $CoV(k_i) = 0.15$ (5000 realizations per k_{mean} value, assuming that k_1 and k_2 are normally distributed*

As shown in Figure 6, the end moments are significantly influenced by stiffness variability, especially for low k_{mean}-values. Low mean connection stiffness values result in greater variability of the end moments. Timber moment-resisting connections are typically semi-rigid with k_{mean}-values up to maximum 5-6 and thus such

variability of the end moments is to be expected. For increasing k_{mean}-values (i.e. quasi-rigid connections) the variability and the 95th/98th percentiles of the end moments reduce significantly. On the other hand, the variabilities and the 95th/98th percentiles of the span moment (Figure 7) and the shear forces (Figure 8) are fairly small and not sensitive to k_{mean}-values.

Tables 1-3 provide the coefficient of variation and the 95th/98th percentiles of the ratios $n_{M,end}$ (Eq.(33) or Eq.(34)), $n_{M,span}$ (Eq.(35)) and $n_{V,end}$ (Eq.(36) or Eq.(37)) for varying values of k_{mean} and CoV(k) based on 5000 realizations.

*Table 1: Coefficient of variation, 95th and 98th percentile of ratio $n_{M,end,i}$ for different mean values and coefficients of variation of the normalized stiffness **k** (assuming that k is normally distributed, based on 5000 realizations)*

$CoV(n_{M,end,i})$					
			$CoV(k)$		
k_{mean}	0.10	0.15	0.20	0.25	0.30
0.5	0.086	0.130	0.172	0.217	0.261
1	0.076	0.114	0.154	0.194	0.242
1.5	0.069	0.105	0.141	0.184	0.221
2	0.066	0.098	0.131	0.169	0.204
3	0.055	0.086	0.115	0.150	0.183
5	0.044	0.067	0.093	0.120	0.151
10	0.030	0.045	0.065	0.086	0.112
15	0.022	0.036	0.048	0.068	0.091
$n_{M,end,i,95\%}$					
			$CoV(k)$		
k_{mean}	0.10	0.15	0.20	0.25	0.30
0.5	1.139	1.208	1.268	1.338	1.404
1	1.118	1.178	1.232	1.283	1.348
1.5	1.110	1.162	1.208	1.259	1.305
2	1.101	1.147	1.188	1.232	1.274
3	1.086	1.127	1.166	1.203	1.241
5	1.067	1.098	1.128	1.153	1.184
10	1.044	1.064	1.087	1.105	1.131
15	1.034	1.050	1.066	1.084	1.101
$n_{M,end,i,98\%}$					
			$CoV(k)$		
k_{mean}	0.10	0.15	0.20	0.25	0.30
0.5	1.173	1.259	1.327	1.412	1.505
1	1.151	1.221	1.284	1.345	1.427
1.5	1.134	1.195	1.257	1.316	1.371
2	1.124	1.176	1.224	1.279	1.327
3	1.106	1.156	1.202	1.250	1.289
5	1.082	1.122	1.154	1.194	1.230
10	1.056	1.080	1.106	1.130	1.160
15	1.042	1.063	1.083	1.106	1.135

The 95th/98th percentiles of $n_{M,end}$ can be approximated by the following expressions:

$$n_{M,end,95\%} \approx 1 + 1.15 \cdot k_{mean}^{-0.35} \cdot CoV(k) \qquad (40)$$

$$n_{M,end,98\%} \approx 1 + 1.40 \cdot k_{mean}^{-0.35} \cdot CoV(k) \qquad (41)$$

*Table 2: Coefficient of variation, 95th and 98th percentile of ratio $n_{M,span}$ for different mean values and coefficients of variation of the normalized stiffness **k** (assuming that k is normally distributed, based on 5000 realizations)*

$CoV(n_{M,span})$					
			$CoV(k)$		
k_{mean}	0.10	0.15	0.20	0.25	0.30
0.5	0.009	0.013	0.018	0.022	0.026
1	0.013	0.020	0.027	0.034	0.042
1.5	0.016	0.024	0.032	0.042	0.051
2	0.018	0.027	0.036	0.046	0.056
3	0.019	0.029	0.039	0.051	0.062
5	0.018	0.028	0.040	0.052	0.064
10	0.015	0.024	0.033	0.045	0.058
15	0.012	0.019	0.026	0.037	0.052
$n_{M,span,95\%}$					
			$CoV(k)$		
k_{mean}	0.10	0.15	0.20	0.25	0.30
0.5	1.015	1.022	1.031	1.038	1.045
1	1.024	1.036	1.050	1.061	1.079
1.5	1.028	1.044	1.059	1.080	1.098
2	1.032	1.049	1.068	1.088	1.112
3	1.034	1.053	1.074	1.105	1.130
5	1.033	1.055	1.078	1.109	1.136
10	1.028	1.045	1.067	1.096	1.127
15	1.023	1.038	1.053	1.079	1.109
$n_{M,span,98\%}$					
			$CoV(k)$		
k_{mean}	0.10	0.15	0.20	0.25	0.30
0.5	1.019	1.028	1.037	1.050	1.058
1	1.029	1.045	1.063	1.078	1.104
1.5	1.035	1.055	1.075	1.107	1.127
2	1.038	1.061	1.086	1.116	1.148
3	1.044	1.069	1.097	1.133	1.172
5	1.040	1.070	1.103	1.145	1.187
10	1.036	1.060	1.092	1.132	1.188
15	1.030	1.049	1.072	1.106	1.165

The 95th/98th percentiles of $n_{M,span}$ can be approximated by the following expressions:

$$n_{M,span,95\%} \approx 1 + (1 - e^{-k_{mean}}) \cdot CoV(k)^{1.45} \qquad (42)$$

$$n_{M,span,98\%} \approx 1 + (1 - e^{-k_{mean}}) \cdot \text{CoV}(k)^{1.30} \quad (43)$$

Table 3: *Coefficient of variation, 95th and 98th percentile of ratio $n_{V,end,i}$ for different mean values and coefficients of variation of the normalized stiffness k (assuming that k is normally distributed, based on 5000 realizations)*

	CoV($n_{V,end,i}$)				
	CoV(k)				
k_{mean}	0.10	0.15	0.20	0.25	0.30
0.5	0.004	0.007	0.009	0.011	0.013
1	0.007	0.010	0.014	0.017	0.021
1.5	0.008	0.012	0.016	0.021	0.025
2	0.009	0.013	0.018	0.023	0.028
3	0.009	0.015	0.020	0.025	0.031
5	0.009	0.014	0.020	0.025	0.031
10	0.007	0.011	0.016	0.022	0.028
15	0.006	0.010	0.013	0.018	0.024

	$n_{V,end,i,95\%}$				
	CoV(k)				
k_{mean}	0.10	0.15	0.20	0.25	0.30
0.5	1.007	1.011	1.014	1.018	1.022
1	1.011	1.017	1.022	1.027	1.035
1.5	1.013	1.020	1.027	1.034	1.042
2	1.015	1.022	1.030	1.038	1.045
3	1.016	1.024	1.032	1.041	1.051
5	1.015	1.023	1.031	1.040	1.051
10	1.012	1.019	1.026	1.034	1.043
15	1.010	1.015	1.022	1.029	1.037

	$n_{V,end,i,98\%}$				
	CoV(k)				
k_{mean}	0.10	0.15	0.20	0.25	0.30
0.5	1.009	1.014	1.018	1.022	1.027
1	1.014	1.020	1.028	1.034	1.043
1.5	1.017	1.026	1.033	1.043	1.052
2	1.018	1.028	1.037	1.049	1.057
3	1.020	1.031	1.042	1.055	1.066
5	1.018	1.030	1.042	1.053	1.067
10	1.016	1.024	1.035	1.046	1.061
15	1.013	1.022	1.029	1.039	1.053

The 95th/98th percentiles of $n_{V,end}$ can be approximated by the following expressions:

$$n_{V,end,95\%} \approx 1 + (0.15 - e^{-5 \cdot k_{mean}}) \cdot \text{CoV}(k) \quad (44)$$

$$n_{V,end,98\%} \approx 1 + (0.20 - e^{-5 \cdot k_{mean}}) \cdot \text{CoV}(k) \quad (45)$$

The relative difference of the 95th/98th percentiles assuming lognormal distribution of the stiffness parameter k is within 6% or less compared to the values in Tables 1-3. This is also indicated by the distribution shape of the output variables, shown in Figure 5.

As shown in the values of Tables 1-3, the ratio $n_{M,end,i}$ (Table 1) is more affected by the variability of the stiffness parameter k. In other words, the end-moments are more sensitive to the stiffness variability compared to the span moment and the shear forces. As expected, the coefficient of variation of the stiffness parameter k results in higher variability of the output variables.

To facilitate comparison, we can consider a connection with $k_{mean} = 1.5$. For $\text{CoV}(k) = 15\%$, the 98th percentile of the end moment, the span moment and the shear force are approx. 20%, 5% and 3% higher than the reference values respectively. The corresponding 98th percentile values for $\text{CoV}(k) = 30\%$ are approx. 37%, 13% and 5%. Especially for the end moments, the 98th percentiles may reach values of the order of 20-40% higher than the reference value for reasonable input ($\text{CoV}(k) \geq 15\%$ and $k_{mean} = 1 - 5$). Such effect should be considered in the design.

4.2 FINITE ELEMENT ANALYSIS OF MOMENT-RESISTING TIMBER FRAMES

The effects of connection stiffness variability are further studied in this Section by use of Finite Element (abbr. FE) analyses of planar MRTFs. The software SAP2000 was used for the structural analysis. An algorithm was developed to perform several analyses with varying properties.

The structural model for the analysis is presented in Figure 9. The frames consisted of glulam columns and beams with cross-sectional dimensions $b_c \times h_c$ and $b_b \times h_b$ respectively. The columns were continuous. The mean modulus of elasticity was $E_{0,mean} = 13000$ N/mm² and the mean shear modulus was $G_{mean} = 650$ N/mm². These values correspond to strength class GL30c [16]. The beams and the columns were modelled as linear elements and the material was modelled as linear-elastic. Shear deformations of timber were taken into account in the model. All frames consisted of 3 bays with 8.0m bay length between the center-lines of the columns. Frames with 4 and 8 storeys were studied. The height of each storey was $h =$ 3.0 m.
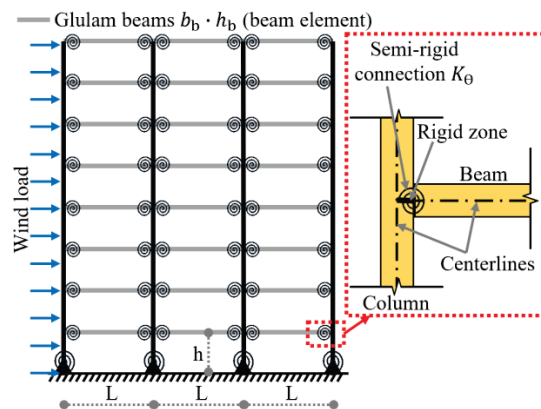

Figure 9: *Structural model for FE analyses*

The connections were modelled as linear-elastic rotational springs with spring constant K_θ (by use of the partial release command of SAP2000). With respect to the translational degrees of freedom, the connections were modelled as rigid. Since the columns were continuous, the connections were placed at the edge of the columns with a rigid offset of $h_c/2$ to the columns' centerline, see the detail in Figure 9. The supports of the frame were assumed rigid with respect to translations while the for the rotational degree of freedom a small rotational stiffness of 5000 kNm/rad was assumed.

Three actions were considered in the analysis: dead load ($G = 2.0$ kN/m^2), live load ($Q = 3.0$ kN/m^2) and the wind action W. The wind load was calculated according to EN 1991-1-4 [17] for a basic wind velocity $v_b = 26$ m/s and terrain category IV (urban environment). For the determination of loads on the frame and wind-induced accelerations it was assumed that the building consists of six frames equally spaced at a distance of 4.0 meters, resulting in a total width of 20 m.

To consider the connection stiffness variability, the stiffness of each beam-to-column connection was selected as a normally distributed random variable (see Eqs.(38)-(39)). Similar to the definition given by Eq.(24), the stiffness can be expressed in dimensionless form by dividing the rotational stiffness by the bending stiffness of the beams, i.e.: $k = K_\theta/(EI_b/L_b)$. Here, L_b is the net bay length. For each frame, analyses with mean dimensionless connection stiffness of $k_{mean} = 1.5$ and $k_{mean} = 2.5$ were performed. These values represent feasible connection stiffness for moment resisting connections with threaded rods (see Section 2). Moreover, they are sufficient, so that the frames fulfil the serviceability requirements with respect to wind-induced deformations and accelerations; see e.g. Figure 10 for accelerations. For each k_{mean}-value, two values of the coefficient of variation were considered: $CoV(K_\theta) = 15\%$ and 25%.

As a crude simplification, the modulus of elasticity and the shear modulus of glulam were assumed constant and equal to their mean value, i.e. their variability was not taken into account in this analysis. All other parameters (e.g. loads, mass etc.) were also kept constant. Therefore, the results of these analyses should only be considered as indicative; however, they allow for comparison with the results provided in Section 4.1. In total, 8 frames were studied (2 number of storeys $\times$ 2 k_{mean}-values $\times$ 2 $CoV(K_\theta)$ values). For each frame type, 3000 realizations were generated and solved by use of FE analysis (in total 24000 analyses were performed).

The following response quantities were quantified by FE analysis, for each frame:

- The internal actions were determined by use of linear-elastic analysis. The envelopes of the internal forces and moments were then determined for the fundamental Ultimate Limit State combinations according to EN1990 [18], with wind load (in both directions) being the leading variable action. The load safety factors were $\gamma_G = 1.2$ for the permanent load, $\gamma_Q = 1.5$ for the live load and $\gamma_W = 1.5$ for the wind load. The ratios between the envelope internal forces and moments for each realization divided by the corresponding values obtained by use of analysis with mean stiffness values were determined for each frame, as specified by Eqs.(33)-(37).

- The horizontal deflections were determined for the characteristic Serviceability Limit State combination according to EN1990 [18], with wind as the leading variable load. The maximum horizontal deflection is denoted Δ and the maximum inter-storey drift is denoted IDR_{max}.

- The fundamental eigenfrequency (f) was quantified by modal analysis. The quasi–permanent load ($G + 0.3 \cdot Q$), according to EN1990 [18] was used to determine the mass.

- The wind-induced accelerations (A) on the top-floor were determined by use of the approximate method given by EN1991-1-4 [17] (Annex B), A damping ratio of $\xi = 2.0$ % was assumed based on measurements of timber buildings [19]. The accelerations were compared to the requirements by ISO10137 [20]. To consider the smaller return period, the basic wind velocity was multiplied by $c_{prob} = 0.73$.

The results of the FE analyses are summarized in Table 4 (4 storey frames) and Table 5 (8 storey frames). The ratios $n_{M,end}, n_{M,span}, n_{V,end}$ (Eqs.(33)-(37)) were determined separately for each connection of the frame and the range is given in the Tables. As indicated by the small ranges the ratios for different connections are quite similar. The FE results can be summarized as follows:

- The end moments are -by far- the action that it is most sensitive to connection stiffness as indicated by the higher $n_{M,end}$-values. On the other hand, the span moments and the shear forces are not very sensitive to connection stiffness as indicated by the low values of $n_{M,span}$ and $n_{V,end}$.

- The ratios $n_{M,end}, n_{M,span}, n_{V,end}$ are quite similar for 4-storey and 8-storey frames. Moreover, they are in very good agreement with the results obtained by the simple beam model in Section 4.1 (Tables 1-3). In fact, the beam model results in slightly higher values of $n_{M,end}$. Therefore, the beam model can be used to provide safe-sided predictions.

- The effect of stiffness variability on deformations, eigenfrequency and top-floor accelerations is quite small as indicated by FE results. Figure 10 shows a plot of the fundamental eigenfrequencies and top floor accelerations for all realizations of MRTFs, compared to ISO10137 [20] requirements. As shown by the results, the response of all realizations is quite similar for each frame. Therefore, the effects of the variability of connection stiffness can be neglected in the serviceability limit state.

The aim of the present -preliminary- study was to highlight the effects of connections' stiffness variability. A more detailed reliability analysis considering the variability of the loads and the material stiffness can be used to better quantify the values of ratios $n_{M,end}, n_{M,span}$

and $n_{V,end}$. Moreover, the presented results come solely from linear-elastic analysis; i.e. possible redistribution of moments if the connections are ductile was not considered.
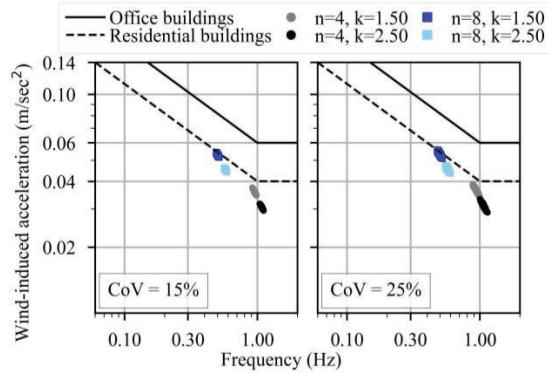
Figure 10: Fundamental eigenfrequency – top floor acceleration for all realizations of MRTFs, compared to ISO10137 [20] requirements

Table 4: FE results of 4-storey MRTFs (3000 realizations per frame)

Frame datails	$N =4$ storeys, $h = 3.0$ m, $H = 12.0$ m			
	3 bays, $L = 8$ m			
	$b_c \times h_c = b_b \times h_b = 430 \times 585$ mm^2			
K_θ (kNm/rad)	18866	18866	31443	31443
k_{mean}	1.5	1.5	2.5	2.5
CoV(k)	15%	25%	15%	25%
CoV($n_{M,end}$)	8-9%	14-16%	6-8%	12-14%
$n_{M,end,95\%}$	1.12-1.14	1.19-1.22	1.09-1.11	1.15-1.17
$n_{M,end,98\%}$	1.15-1.17	1.23-1.27	1.11-1.14	1.18-1.21
CoV($n_{M,span}$)	≈2%	3-4%	2-3%	4-5%
$n_{M,span,95\%}$	1.03-1.05	1.06-1.09	1.04-1.05	1.08-1.10
$n_{M,span,98\%}$	1.05-1.06	1.09-1.12	1.05-1.07	1.10-1.13
CoV($n_{V,end}$)	1%	1-2 %	1%	1-2 %
$n_{V,end,95\%}$	1.01-1.02	1.02-1.03	1.01-1.02	1.02-1.03
$n_{V,end,98\%}$	1.02	1.03-1.05	1.02	1.03-1.05
Δ_{mean} (mm)	6.73	6.81	5.13	5.16
CoV(Δ_{max})	9%	15%	9%	16%
mean(IDR_{max}) (mm)	2.71	2.74	2.25	2.26
CoV(IDR_{max})	6%	11%	6%	11%
f_{mean} (Hz)	0.950	0.946	1.080	1.075
CoV(f)	1%	2%	1%	2%
A_{mean} (m/s^2)	0.036	0.036	0.030	0.031
CoV(A)	1%	2%	1%	2%

Table 5: FE results of 8-storey MRTFs (3000 realizations per frame)

Frame datails	$N =8$ storeys, $h = 3.0$ m, $H = 24.0$ m			
	3 bays, $L = 8$ m			
	$b_c \times h_c = b_b \times h_b = 430 \times 585$ mm^2			
K_θ (kNm/rad)	18866	18866	31443	31443
k_{mean}	1.5	1.5	2.5	2.5
CoV(k)	15%	25%	15%	25%
CoV($n_{M,end}$)	8-9%	14-16%	6-8%	12-14%
$n_{M,end,95\%}$	1.11-1.14	1.19-1.23	1.09-1.11	1.14-1.18
$n_{M,end,98\%}$	1.14-1.17	1.23-1.27	1.11-1.13	1.17-1.22
CoV($n_{M,span}$)	≈2%	3-5%	2-3%	4-5%
$n_{M,span,95\%}$	1.03-1.06	1.07-1.12	1.04-1.07	1.08-1.13
$n_{M,span,98\%}$	1.04-1.08	1.09-1.15	1.05-1.08	1.10-1.17
CoV($n_{V,end}$)	≈1%	1-2%	≈1%	≈2%
$n_{V,end,95\%}$	1.01-1.02	1.02-1.03	1.01-1.02	1.02-1.03
$n_{V,end,98\%}$	1.02	1.03-1.04	1.02	1.03-1.04
Δ_{mean} (mm)	35.26	35.70	26.39	26.69
CoV(Δ_{max})	3%	5%	3%	5%
mean(IDR_{max}) (mm)	8.49	8.55	6.84	6.92
CoV(IDR_{max})	3%	5%	3%	5%
f_{mean} (Hz)	0.501	0.498	0.577	0.574
CoV(f)	1%	1%	1%	1%
A_{mean} (m/s^2)	0.053	0.053	0.045	0.045
CoV(A)	1%	1%	1%	1%

5 CONCLUSIONS AND FUTURE WORK

This paper provides an overview of analysis and design aspects of moment-resisting connections with inclined threaded rods. In the first part of the paper, a series of expressions that estimate the properties of such connections were provided based on recent publications. In the second part of the paper, a preliminary study on the effect of connections' stiffness variability on the structural response of timber frames was presented, based on a simple beam model and Finite Element simulations of planar frames. In common practice, structural analysis of timber structures is performed by use of mean stiffness values. However, in moment-resisting frames the magnitude and distribution of internal forces and moment is highly dependent on the stiffness of their connections. The results of this study have shown that the variability of connections' stiffness can result in great variability of the internal forces and moments. The end moments are more sensitive to this effect with 98th percentiles of the order of 20%-40% higher than the reference values obtained by analysis with mean stiffness values. Such increase should be considered in the design for the Ultimate Limit State. The Finite element results were in good agreement with the predictions obtained by use of a simple beam model

with rotational springs. When it comes to serviceability requirements, the FE models showed that the variability of connections' stiffness has small influence and may be neglected.

REFERENCES

[1] A. Vilguts, H. Stamatopoulos, and K. A. Malo, "Parametric analyses and feasibility study of moment-resisting timber frames under service load," *Engineering Structures,* vol. 228, p. 111583, 2021/02/01/ 2021, doi: https://doi.org/10.1016/j.engstruct.2020.111583 .

[2] K. Lied and K. Nordal, "A conceptual study of glulam connections using threaded rods and connecting circular steel profiles," in "Master thesis," NTNU Norwegian University of Science and Technology, Trondheim, Norway, 2016.

[3] A. Vilguts, S. Ø. Nesheim, H. Stamatopoulos, and K. A. Malo, "A study on beam-to-column moment-resisting timber connections under service load, comparing full-scale connection testing and mock-up frame assembly," *European Journal of Wood and Wood Products,* vol. 80, no. 4, pp. 753-770, 2022/08/01 2022, doi: 10.1007/s00107-021-01783-2.

[4] H. Stamatopoulos, K. A. Malo, and A. Vilguts, "Moment-resisting beam-to-column timber connections with inclined threaded rods: Structural concept and analysis by use of the component method," *Construction and Building Materials,* vol. 322, p. 126481, 2022, doi: https://doi.org/10.1016/j.conbuildmat.2022.126 481.

[5] R. Steiger and E. Gehri, "Interaction of shear stresses and stresses perpendicular to grain," presented at the Proceedings of the 44th CIB-W18 meeting, Alghero, Italy, 2011.

[6] P. Dietsch, H. Kreuzinger, and S. Winter, "Design of shear reinforcement for timber beams," presented at the Proceedings of the 46th CIB-W18 meeting Vancouver, Canada, 2013.

[7] H. Stamatopoulos and K. A. Malo, "On strength and stiffness of screwed-in threaded rods embedded in softwood," *Construction and Building Materials,* vol. 261, p. 119999, 2020/11/20/ 2020, doi: https://doi.org/10.1016/j.conbuildmat.2020.119 999.

[8] H. J. Blaß and O. Krüger, *Schubverstärkung von Holz mit Holzschrauben und Gewindestangen*. Karlsruhe: KIT Scientific Publishing, 2010.

[9] H. Stamatopoulos and K. A. Malo, "Withdrawal stiffness of threaded rods embedded in timber elements," *Construction and Building Materials,* vol. 116, pp. 263-272, 2016, doi: http://dx.doi.org/10.1016/j.conbuildmat.2016.04 .144.

[10] H. Stamatopoulos and K. A. Malo, "Withdrawal capacity of threaded rods embedded in timber elements," *Construction and Building Materials,*
vol. 94, pp. 387-397, 2015, doi: http://dx.doi.org/10.1016/j.conbuildmat.2015.07 .067.

[11] H. Stamatopoulos, F. M. Massaro, and J. Qazi, "Mechanical properties of laterally loaded threaded rods embedded in softwood," *European Journal of Wood and Wood Products,* 2021/09/15 2021, doi: 10.1007/s00107-021-01747-6.

[12] CEN, "NS-EN 1995-1-1:2004+A1:2008+A2:2014+NA:2010," in *Design of timber structures - Part 1-1: General - Common rules and rules for buildings*, ed. Brussels: European committee for standarization, 2004.

[13] T. Laggner, G. Flatscher, and G. Schickhofer, "Combined loading of self-tapping screws," presented at the Proceedings of WCTE 2016 - World Conference on Timber Engineering, Vienna, Austria, 2016.

[14] S. Aicher and K. Simon, "Rigid Glulam Joints with Glued-in Rods subjected to Axial and Lateral Force Action," presented at the Proceedings of the 8th INTER meeting Karlsruher Institut für Technologie (KIT), 2021.

[15] A. Vilguts, "Moment-resisting timber frames with semi-rigid connections," Ph.D. Thesis, Department of Structural Engineering, Norwegian University of Science and Technology, Trondheim, Norway, 2021.

[16] CEN, "EN 14080-2013: Timber structures-Glued laminated timber and glued solid timber - Requirements," ed. Brussels, Belgium: European Committee for Standardization, 2013.

[17] CEN, "NS-EN 1991-1-4:2005+NA:2009," in *Actions on structures - Part 1-4: General actions - Wind actions*, ed. Brussels, Belgium: European Committee for Standardization, 2009.

[18] CEN, "NS-EN 1990:2002+A1:2005+NA:2016," in *Basis of structural design*, ed. Brussels, Belgium: European Committee for Standardization, 2016.

[19] A. Feldmann *et al.*, "Dynamic properties of tall timber structures under wind-induced vibration," presented at the Proceedings of WCTE 2016 - World Conference on Timber Engineering, Vienna, Austria, 2016.

[20] ISO, International Organization for standardization, "ISO10137: Bases for design of Structures - Serviceability of Buildings and Walkways against Vibrations," ed. Geneva, Switzerland: ISO, 2007.